Maternal obesity may disrupt offspring metabolism by inducing oocyte genome hyper-methylation via increased DNMTs

Shuo Chao[1#], Jun Lu[1#], Li-Jun Li[1], Hong-Yan Guo[1], Kui-Peng Xu[2], Ning Wang[1], Shu-Xian Zhao[1], Xiao-Wen Jin[1], Shao-Ge Wang[1], Shen Yin[1], Wei Shen[1], Ming-Hui Zhao[1], Gui-An Huang[1], Qing-Yuan Sun[3*], Zhao-Jia Ge[1*]

1. College of Life Sciences, Institute of Reproductive Sciences, Key Laboratory of Animal Reproduction and Germplasm Enhancement in Universities of Shandong, Qingdao Agricultural University, Qingdao 266109, P.R. China;

2. College of Horticulture, Qingdao Agricultural University, Qingdao 266109, P.R. China;

3. Guangzhou Key Laboratory of Metabolic Diseases and Reproductive Health, Guangdong-Hong Kong Metabolism & Reproduction Joint Laboratory, Reproductive Medicine Center, Guangdong Second Provincial General Hospital, Guangzhou 510317, China.

# These authors have equal contributions to this work.

* Corresponding author: Zhao-Jia Ge

College of Life Sciences, Qingdao Agricultural University,

Qingdao 266109, P.R. China; +86 15588647272

Emails: gejdssd313@163.com; zjge@qau.edu.cn

Qing-Yuan Sun

Reproductive Medicine Center, Guangdong Second Provincial General Hospital, Guangzhou 510317, China. sunqy@gd2h.org.cn

Abstract

Maternal obesity has deleterious effects on oocyte genome methylation establishment, yet the underlying mechanisms remain unclear. In the present study, we first find that maternal obesity induced by high-fat diet (HFD) disturbs genomic methylation in oocytes, and at least a part of the altered methylation is transmitted to F2 oocytes and livers via females. We further identified that altered metabolites such as methionine and melatonin may play a key role in the re-methylation establishment in oocytes of obese mice. Exogenous melatonin treatment significantly reduces the hyper- methylation of HFD oocytes. The higher expression of DNMT3a and DNMT1 in HFD oocytes is also decreased by melatonin supplement, which may be mediated by cAMP/PKA/CREB pathway. These results suggest that maternal obesity-induced genomic methylation alterations in oocytes, can be partly transmitted to F2 in females, and that melatonin is involved in regulating the hyper-methylation of HFD oocytes via increasing the expression of DNMTs mediated by cAMP/PKA/CREB pathway.

Key words: Obesity, oocyte, methylation, melatonin, cAMP/PKA/CREB pathway

Introduction

Obesity has become a global health problem, affecting about 13% of the world's adult population, and more than 340 million children and adolescence (WHO). Obesity has negative effects on reproduction and offspring health. It's demonstrated that maternal obesity not only reduces the function of the hypothalamic-pituitary-ovarian (HPO) axis (*1*), oocyte cytoplasmic quality, and nuclear maturation, but also induces abnormal genome methylation (*2*). Reduced expression of *Stella* in oocytes induced by obesity results in global hypo-methylation in zygotes, which is an important contribution to the defective embryo development (*3*). Offspring of obese females also shows a higher risk of non-communicable diseases, such as obesity, diabetes, and cardiovascular diseases (*4*). Our previous study demonstrates that obesity altered the methylation level of *Leptin*, which might play a role in the metabolic disorders of female offspring, but the abnormal methylation of *Leptin* is not observed in F1 oocytes (*5*). The influence of maternal obesity on genomic methylation of oocytes is still obscure. Therefore, more studies are necessary to explore the role of methylation in mediating the transgenerational transmission of metabolic syndrome induced by female obesity.

Obesity results in abnormalities of glucose and lipid metabolism, which has negative effects on oocyte maturation and embryo development. In obese females, the circulating free fatty acids level is higher, which induces

65 lipotoxicity to oocytes. The mitochondrial function of oocytes from obese
66 females is also decreased (*2*). These indicate that the disturbed metabolism
67 induced by obesity plays a key role in the reduced oocyte quality. Therefore,
68 we suppose that disturbed metabolism induced by obesity may be an
69 important reason for the abnormal methylation in oocytes.
70 In the present study, we investigated the effects of metabolites in obese
71 mice on genomic methylation of oocytes and its inheritance via females.

72 **Results**

73 **Obesity alters genomic methylation in oocytes**

74 Obese mouse model was induced by feeding high-fat diet (HFD) (*3, 5*),
75 and mice fed with normal diet was used as a control (CD). The average
76 body weight of HFD group was significantly higher than that in the CD
77 group (n>86, Fig. S1A and B). Re-methylation in oocytes occurs in
78 follicular development and is nearly completed at the germinal vesical
79 stage (GV). The 5mC (5-methylcytosine) and 5hmC (5-
80 hydroxymethylcytosine) levels in the GV oocytes of HFD mice were
81 significantly higher than in the CD group (n>30, Fig. 1A-C). To further
82 explore the effects of maternal obesity on oocyte methylation, we
83 examined the genomic methylation of metaphase II (MII) oocytes using
84 whole genome bisulfite sequencing for small samples (WGBS, Novogene,
85 Beijing, China). Results showed that the global methylation in MII oocytes
86 of HFD group was higher than that in the CD group (Fig. 1D). Methylated

87 cytosine (C) showed three types in the genome including CG, CHG and
88 CHH (H=A, T or C), and methylated CG had more contribution in
89 regulating gene expression. Therefore, we further analyzed the CG
90 methylation in the present study. We found that the CG methylation level
91 in HFD MII oocytes was significantly higher than that in the CD group
92 (Fig. 1E). Differentially methylated CG distributed at all chromosomes
93 (Fig. S1C). To further analyze the distribution of methylation, each
94 function region of gene was equally divided into 20 bins, and then the
95 average methylation levels of function regions of all genes were calculated,
96 respectively. CGIs (CG islands) and CGI shore were predicted using
97 cpgIslandExt and repeat sequences were predicted using RepeatMasker.
98 Results showed that hyper-methylation was mainly distributed at promoter,
99 exon, upstream 2k, and downstream 2k regions (Fig. 1F and Fig. S1D) in
100 oocytes of obese mice.

101 **Distribution of differentially methylated regions (DMRs)**

102 We further analyzed the differentially methylated regions (DMRs) in
103 oocytes of both HFD and CD groups, and identified 4340 DMRs at the
104 standards: the number of CG ≥4 and the absolute methylation difference ≥
105 0.2, including 2013 hyper-DMRs (46.38%) and 2327 hypo-DMRs (53.62%)
106 (Fig. 1G), which distributed at all chromosomes (Fig. 1H). We then
107 annotated DMRs into different genomic regions including promoter, exon,
108 intron, CGI, CGI shore, repeat, TSS (transcription start site), TES

109 (transcription end site), UTR3 (3' end untranslated region), and UTR5 (5'
110 end untranslated region) (Fig. S2A), and the average methylation level of
111 DMRs in these regions were similar between HFD and CD oocytes (Fig.
112 S2B). Methylation level at promoters has great contributions in regulating
113 gene expression. We then analyzed the enrichment of genes with DMRs at
114 promoters in KEGG (Kyoto Encyclopedia of Genes and Genomes)
115 pathways using KOBAS online. Results indicated that genes with DMRs
116 at promoters were significantly enriched in metabolic pathways including
117 amino acid metabolism pathways, carbohydrate metabolism pathways,
118 lipid metabolism pathways, metabolism of cofactors and vitamins
119 pathways, and so on (Fig. 1I, Table S1). A total of 35 genes with DMRs
120 at promoters were included in metabolism pathways, and 19 genes were
121 with hyper-DMRs and 16 genes were with hypo-DMRs (Table S2). These
122 results suggest that the altered methylation in oocytes induced by maternal
123 obesity may play a role in the offspring metabolic disorders.

124 **Disturbed methylation can be inherited transgenerationally through**
125 **females**

126 Both oocyte quality and uterine environment have contributions to adult
127 diseases that may be mediated by epigenetic modifications (*6*). Our recent
128 study demonstrates that disturbed methylation in oocytes caused by uterine
129 undernourishment can be partly transmitted to F2 oocytes via female,
130 which may play a key role in the transgenerational inheritance of metabolic

131 disorders (*7*). To investigate the inheritance of altered methylation in
132 oocytes, we bred F1 and F2 generations as shown in Fig. 1J: F1, female
133 HFD (HF1) and CD (CF1) respectively mated with control male; F2,
134 female HF1 (HF2) and CF1 (CF2) respectively mated with control male.
135 We examined the glucose and insulin tolerance (GTT and ITT), and results
136 showed that the impaired GTT and ITT w in F0, F1, and F2 females (Fig.
137 2A-C).
138 To confirm the transmission of disturbed methylation via females, we
139 examined the methylation status of some DMRs located at promoters of
140 *Bhlha15* (also known as *Mist1*, basic helix-loop-helix, a transcriptional
141 factor), *Mgat1* (mannoside acetylglucosaminyltransferase 1), T*aok3*
142 (Serine/threonine-protein kinase 3), *Tkt* (transketolase), *Pik3cd*
143 (phosphatidylinositol-4, 5-bisphosphate 3-kinase catalytic subunit delta),
144 and *Pld1* (phospholipase D1). We found that the methylation levels of
145 hyper-DMRs including *Bhlha15*-DMR, *Mgat1*-DMR, and *Taok3*-DMR in
146 HFD oocytes were significantly higher than in the CD group (Fig. 2D); the
147 methylation level of hypo-DMRs *Pik3cd-DMR* in HFD oocytes was
148 significantly lower than that in the CD group (Fig. 2D). These results
149 coincide with the genomic sequencing results. But the methylation level of
150 *Tkt-DMR* (hypo-DMR) in HFD oocytes was higher than that in the CD
151 group, and the methylation level of *Pld1-DMR* (hypo-DMR) was similar
152 between two groups, which were contradictory with the genomic

153 sequencing results (Fig. S3A). These results suggest that some regions are
154 false-positive in genomic sequencing result. To exclude the effects of
155 somatic cell contamination, we examined the methylation level of
156 paternally imprinted gene *H19,* and it was low in both HFD and CD
157 oocytes (Fig. S3B). This indicates that samples are not contaminated by
158 somatic cells.

159 If the altered methylation in oocytes induced by obesity would transmit to
160 offspring, it would be found in tissues. We then examined the methylation
161 status of DMRs in F1 livers using bisulfite sequencing (BS). Ten livers
162 from five litters were analyzed for each group. Results showed that the
163 methylation levels of *Bhlha15*-DMR and *Mgat1*-DMR were higher and the
164 methylation of *Pik3cd*-DMR was lower in livers of HF1 (Fig. S4A-C) ,
165 which coincides with that in HFD oocytes. The methylation level of *Tkt-*
166 *DMR* in HF1 livers was lower than that in CF1 (Fig. S4D), although it was
167 higher in HFD oocytes. This indicates that the uterine environment of
168 obesity and reprogramming may also have contributions to this
169 contradiction. We further examined the expression of genes with DMRs at
170 promoters, including hyper-methylated genes, *Bhlha15*, *Mgat1*, *Dgka*,
171 *Pdpk1* and *Taok3*, and hypo-methylated genes, *Igf1*, *Map3k8*, *Pld1*, *Tkt*,
172 *Pik3cd* and *Sphk2*. The expressions of *Bhlha15*, *Mgat1* and *Pdpk1* were
173 significantly lower and the expression of *Map3k8*, *Tkt*, *Pik3cd*, and *Sphk2*
174 were significantly higher in HF1 livers compared with CF1 group (Fig.

175 S4E and F). The expression trends of *Bhlha15*, *Mgat1*, *Tkt*, and *Pik3cd*
176 were coincide with the methylation status at promoters in HF1 livers. The
177 expressions of *Dgka*, *Taok3*, *Igf1*, and *Pld1* were not affected in HF1 livers
178 (Fig. S4E and F). *Mgat1* is associated with lipid metabolism and obesity
179 (*8, 9*), *Tkt* regulates glucose metabolism (*10, 11*), and *Pik3cd* is involved
180 in lipid metabolism and diabetes (*12, 13*). These results suggest that the
181 altered methylation in HFD oocytes is partly transmitted to F1 livers via
182 oocytes, and abnormal methylation may be a reason for the disturbed
183 metabolism of HF1.
184 If the altered methylation in HFD oocytes were inherited by HF1 oocytes,
185 it would be transmitted to F2 generation. Therefore, we examined the
186 methylation of DMRs in HF1 oocytes, and results showed that *Bhlha15*-
187 DMR, *Mgat1*-DMR, and *Taok3*-DMR were significantly hyper-methylated
188 in HF1 oocytes compared with CF1 group (Fig. 2E). The methylation level
189 of *Tkt*-DMR was significantly lower (Fig. S5) and the methylation level of
190 *Pik3cd*-DMR was slightly lower in HF1 oocytes than that in CF1 group
191 (Fig. 2E). These results indicate that at least a part of the altered
192 methylation in HFD oocytes is transmitted to F1 oocytes via females.
193 Therefore, we further produced F2 using female HF1 and CF1 to research
194 the transgenerational transmission of disturbed methylation in HFD
195 oocytes (Fig. 1J). The methylation levels of *Bhlha15*-DMR and *Mgat1*-
196 DMR were higher and the methylation level of *Pik3cd*-DMR was lower in

197 HF2 livers compared with CF2 group (Fig. S6A-C). The methylation of
198 *Tkt*-DMR in HF2 livers was similar to CF2 group (Fig. S6D). In addition,
199 the expressions of *Bhlha15*, *Pdpk1*, and *Mgat1* were significantly lower
200 (Fig. S6E), and the expressions of *Pld1*, *Pik3cd*, and *Sphk2* were
201 significantly higher in HF2 livers compared with CF2 group (Fig. S6F).
202 The other genes' expressions were similar in livers between HF2 and CF2
203 groups (Fig. S6E and F). These results suggest that at least a part of the
204 altered methylation in HF2 livers may be inherited from HFD oocytes,
205 which is associated with the altered expressions of genes.
206 Results in Fig. S6 showed that at least a part of the altered methylation in
207 DMRs was transmitted to F2 livers via female. Thus, we supposed that the
208 altered methylation can be, at least partly, inherited by F2 oocytes. We then
209 examined the methylation of DMRs in F2 oocytes using BS, and found that
210 the hyper-methylation of *Bhlha15*-DMR, *Mgat1*-DMR, and *Taok3*-DMR,
211 and the hypo-methylation of *Pik3cd*-DMR and *Tkt*-DMR were maintained
212 in HF2 oocytes compared with CF2 group (Fig. 2F). These results indicate
213 that HF2 oocytes may inherit, at least partly, the altered methylation in
214 HFD oocytes via females.
215 To better understand the inheritance of the altered methylation in HFD
216 oocytes, we systematically analyzed the methylation status in different
217 generations (Fig. 2G). For hyper-DMRs, the hyper-methylation of
218 *Bhlha15*-DMR was maintained from HFD oocytes to F2 oocytes, and the

219 hyper-methylation of *Mgat1*-DMR and *Taok3*-DMR was partly transmitted
220 to F2 from HFD oocytes. For hypo-DMRs, the hypo-methylation of *Tkt*-
221 DMR was partly maintained from F1 to F2, and the hypo-methylation of
222 *Pik3cd*-DMR in HFD oocytes was inherited by F2 (Fig. 2G). For *Pld1*-
223 DMR, the methylation level was similar between CD and HFD oocytes. So
224 we didn't further examined it in F1 and F2 (Fig. 2G). These results suggest
225 that only a part of the altered methylation in HFD oocytes can be
226 transmitted to F2 oocytes, and the disturbed methylation may be a reason
227 for the inheritance of metabolic disorders.

228 **Obesity alters the metabolomics of serum**

229 Obesity alters the metabolism of glucose, fatty acid, and amino acids,
230 which are essential for oogenesis. Thus, we suppose the altered metabolism
231 may play a key role in the disturbed global methylation in HFD oocytes.
232 We examined the metabolomics of serum using non-target approaches
233 (BGI, Wuhan, China). We used LC-MS/MS to identify the variation of
234 metabolites including amino acids, carbohydrates, lipid, phenols, and so on.
235 The principal component analysis (PCA) showed that the PC1 and PC2,
236 respectively, explained 44.6% and 9.96% of the total metabolite variations
237 (Fig. 3A). The distribution of extracts between groups was distinguishable
238 (Fig. 3A). We identified 538 differential metabolites based on the PLS-DA
239 (robust orthogonal partial least squares-discriminant analysis) and T-test
240 was used for analysis: VIP (variable importance in projection)⩾1, Fold-

241 change⩾1.2 or ⩽0.83, and p-value<0.05, including 288 up-regulated and
242 250 down-regulated (Fig. 3B). The enrichment of differential metabolites
243 was analyzed using KEGG and found that differential metabolites were
244 significantly enriched in tryptophan and vitamin B6 metabolism (Fig. 3C).
245 The top 20 differential metabolites were presented in Fig. 3D. These results
246 suggest that obesity disturbs the metabolomics of serum.

247 **Melatonin may play a key role in the genomic hyper-methylation of**
248 **HFD oocytes**

249 To investigate the association between metabolites and methylation, we
250 identified some differential metabolites in HFD mice, including pyridoxine
251 (vitamin B6), L-methionine, melatonin, and L-tyrosine that may be
252 associated with hyper-methylation of oocytes. The concentrations of
253 pyridoxine (vitamin B6), L-methionine, and L-tyrosine were significantly
254 increased in HFD serum compared with the CD group (Fig. 3D-G). In the
255 methionine cycle, methionine adenosyltransferase catalyzes methionine
256 and ATP into S-adenosyl methionine (SAM) (*14*) which acts as a universal
257 methyl donor (*15*). DNA methyltransferases (DNMTs) transfer the methyl
258 group to cytosine and convert SAM to S-adenosyl homocysteine (SAH)
259 which is further degraded to homocysteine (HCY) by SAH hydrolase (*16*).
260 During these processes, vitamin B6 serves as a co-factor (*17*). It's reported
261 that excessive methionine and vitamin B6 intake induces hyper-
262 methylation (*18*). This indicates that the hyper-methylation in HFD oocytes

263 may be associated with the higher concentration of methionine and
264 pyridoxine. To confirm this hypothesis, we examined the concentration of
265 SAM, SAH, and HCY in livers and oocytes, which are crucial intermediate
266 metabolites in methionine cycle. Results showed that the concentrations of
267 SAM, SAH, and HCY in HFD livers were similar to that in CD livers (Fig.
268 3H-J), and the concentration of SAM in HFD oocytes was lower than that
269 in the CD group (Fig. 3K). These results suggest that the higher
270 concentrations of methionine and pyridoxine in serum of HFD mice may
271 be not the main reason for the genomic hyper-methylation in oocytes.
272 As presented in Fig. 3D and L, the concentration of melatonin in HFD
273 serum was significantly lower than that in the CD group. Low
274 concentration of melatonin is also reported in obese rats (*19*) and humans
275 (*20*). Exogenous melatonin supplementation reduces body weight and
276 improves lipid and glucose metabolism in animals and humans (*21*).
277 Melatonin also can inhibit cancer by regulating DNA methylation status
278 (*22*), improve DNA methylation reprogramming in development of porcine
279 cloned embryos (*23*), and affect DNA re-methylation in oocytes (*24-26*).
280 This indicates that the reduced melatonin may contribute to the hyper-
281 methylation of HFD oocytes. In the present study, we found that if HFD
282 mice were treated with exogenous melatonin for 14 days, the genomic
283 hyper-methylation in HFD oocytes was significantly reduced (n≥96 Fig.
284 3M and N). These results suggest that the reduced melatonin concentration

285 may be involved in regulating the hyper-methylation in HFD oocytes.

286 **Melatonin regulates genomic methylation of oocytes by increasing the**
287 **expression of DNMTs via cAMP/PKA/CREB pathway**

288 Melatonin receptors (MT1 and 2), which couples with inhibitor G-protein
289 (Gi), are identified in oocytes and granulosa cells (*27, 28*). The activated
290 Gi inhibits the activation of adenylyl cyclases (ADCYs), resulting in
291 decrease of cAMP (cyclic adenosine monophosphate), which regulates the
292 activation of protein kinase A (PKA) and CREB (cAMP response element-
293 binding protein) (*29*). Elevated cAMP level increases the expression of
294 DNMTs resulting in hyper-methylation in HL-1 cardiomyocytes (*30*).
295 Hedrich *et al*. report that CREMα induces hyper-methylation of CD8
296 cluster via increasing the expression of DNMT3a (*31*). We thus supposed
297 that melatonin may regulate genomic methylation in oocytes via increasing
298 the expression of DNMTs through cAMP/PKA/CREB pathway (Fig. 4A).
299 To confirm this hypothesis, female C57BL/6 mice fed with normal diet
300 were treated with luzindole, an inhibitor of melatonin receptor, and the
301 global methylation of 5mC and 5hmC was significantly increased in
302 oocytes (n≥49 Fig. 4B-D). Luzindole didn't affect the concentration of
303 melatonin in serum (Fig. S7A). However, excessive melatonin treatment
304 significantly increased the concentration of melatonin in serum (Fig. S7A)
305 and decreased the methylation level of 5mC and 5hmC in oocytes (Fig. 4B-

306 D). These indicate that melatonin may regulate re-methylation process in
307 oocytes.
308 To confirm whether melatonin regulates methylation in oocytes via cAMP
309 pathway, we examined the expression of ADCYs in oocytes using RT-PCR,
310 and found that ADCY5, 6, and 9 were expressed in oocytes (Fig. S7B).
311 Melatonin antagonist luzindole significantly increased the expression of
312 ADCY6 and ADCY9 in oocytes, and melatonin reduced the expression of
313 ADCY6 (Fig. 4E). However, the expression of ADCY5 was lower in
314 luzindole and melatonin groups compared with the control (Fig. 4E). In
315 addition, melatonin antagonist luzindole increased while melatonin
316 decreased the concentration of cAMP in oocytes, respectively (Fig. 4F).
317 These results suggest that melatonin may regulate the synthesis of cAMP
318 via ADCY6 in oocytes. To further confirm the role of cAMP in regulating
319 methylation of oocytes, we treated mice with SQ22536, an inhibitor of
320 ADCYs, and showed that this treatment significantly reduced the global
321 methylation of 5mC and the concentration of cAMP in oocytes (n≥51 Fig.
322 5A-C). Whereas, the ADCYs activator forskolin significantly increased the
323 cAMP concentration and global methylation of 5mC in oocytes (Fig. 5A-
324 C). 8-Bromo-cAMP, a cAMP analogue, also increased the global
325 methylation in oocytes (n≥41 Fig. 5D, E). cAMP has function by activating
326 the downstream protein PKA. When we treated mice with H89 2HCL, a
327 PKA antagonist, the global methylation of 5mC was significantly reduced

328 in oocytes (n≥24 Fig. 5F, G). These results suggest that melatonin may
329 mediate methylation of oocytes via cAMP/PKA pathway.
330 cAMP activates PKA which further phosphorylates CREB to regulate gene
331 expression. In oocytes, DNA re-methylation is regulated by DNMTs
332 including DNMT3a, DNMT3l, and DNMT1. Therefore, we next
333 investigated whether melatonin regulates DNMTs expression via
334 cAMP/PKA/CREB pathway in oocytes. We examined the expression of
335 CREB1, CREM (cAMP responsive element modulator), CREB3l2 (cAMP
336 responsive element binding protein 3 like 2), and ATF1 (activating
337 transcription factor 1) in oocytes. Results showed that ADCYs activator
338 forskolin treatment significantly increased the mRNA expression of
339 CREB1 and CREM, and the expression of CREB3l2 and ATF1 was slightly
340 increased (Fig. 6A). In addition, ADCYs inhibitor SQ22536 significantly
341 reduced the expression of CREB1 and CREB3l2, although the expression
342 of CREM and ATF1 was slightly decreased in oocytes (Fig. 6A).
343 Furthermore, ADCYs inhibitor SQ22536 treatment significantly reduced
344 the concentration of pCREB1, but it was increased by forskolin treatment
345 in oocytes (n≥36 Fig. 6B, C). pCREB1 level was also increased by 8-
346 Bromo-cAMP and decreased by PKA antagonist H89 2HCL in oocytes
347 (n≥28 Fig. 6D-G). These suggest that the expression and phosphorylation
348 of CREB1 can be regulated by cAMP/PKA pathway. Yang *et al.*
349 demonstrate that CREB regulates DNMT3a expression in neurons of the

350 dorsal root ganglion via binding to the promoter region (*32*). In the present
351 study, the binding of pCREB1 with relative regions of DNMTs was
352 examined using CUT & Tag assay. Each sample contained 500 GV oocytes,
353 and two replicates were involved. Sequencing result revealed that five
354 fragments including 10 pCREB1 binding motifs (predicted using online
355 tool JASPAR, Table S3) were associated with DNMTs, including 3
356 fragments at intron 1 and distill intergenic regions of DNMT3a, 1 fragment
357 at promoter region of DNMT1, and 1 fragment at intron 13 of DNMT3l
358 (Table S4). These results suggest that pCREB1 may have contributions to
359 regulate the expression of DNMTs.
360 Next, we investigated the expression of DNMT1, DNMT3a, and DNMT3l
361 in oocytes. Melatonin inhibitor luzindole (slightly) and ADCYs activator
362 forskolin (significantly) increased the expression of DNMT1 and DNMT3a,
363 respectively (Fig. 7A, B). Melatonin and ADCYs inhibitor SQ22536
364 significantly and slightly reduced the expression of DNMT1 and DNMT3a
365 in oocytes, respectively (Fig. 7A, B). The protein level of DNMT3a in GV
366 oocytes was also significantly increased by 8-Bromo-cAMP and decreased
367 by PKA antagonist H 89 2HCL, respectively (n≥48 Fig. 7C-F). Although
368 DNMT1 is well known as maintenance methyltransferase, it also has
369 contribution to *de novo* methylation in oocytes (*33*). Therefore, we
370 examined the localization of DNMT1 in oocytes, and found that 8-Bromo-
371 cAMP treatment significantly increased the localization of DNMT1 in the

372 nucleus of oocytes, but it was reduced by PKA antagonist H89 2HCL (n≥22
373 Fig. 7G-J). When the activation of DNMTs was inhibited by 5-azacytidine,
374 the methylation level in GV oocytes was significantly decreased (n≥43 Fig.
375 S8). These results suggest that melatonin may influence the genomic
376 methylation of oocytes via regulating the expression of DNMT1 and
377 DNMT3a mediated by cAMP/PKA/CREB pathway.

378 **Increased DNMTs mediates hyper-methylation of HFD oocytes via**
379 **cAMP/PKA/CREB pathway**

380 To explore how melatonin regulates the hyper-methylation of HFD oocytes,
381 we examined the expression of DNMTs. Results showed that maternal
382 obesity in mice significantly increased the expression of DNMT1,
383 DNMT3a, and DNMT3l in oocytes (Fig. 8A). So, we would like to confirm
384 whether cAMP/PKA/CREB pathway mediated the increased expression of
385 DNMTs in HFD oocytes. We examined the concentration of cAMP in
386 oocytes, and found that maternal obesity significantly increased the
387 concentration of cAMP in oocytes compared with CD group (Fig. 8B). The
388 mRNA expression of CREB1, but not CREM, in HFD oocytes was
389 significantly increased compared with CD group (Fig. 8C), and the
390 pCREB1 level in HFD oocytes was also significantly increased (n≥49 Fig.
391 8D, E). But the higher level of pCREB1 was reduced by exogenous
392 melatonin treatment (Fig. 8D, E). When obese females were treated with
393 PKA antagonist H89 2HCL, both 5mC and pCREB1 levels were

394 significantly reduced in oocytes (n≥17 Fig. 8F-I). These results suggest that
395 reduced melatonin in obese mice may increase the expression of DNMTs
396 by cAMP/PKA/CREB pathway.
397 The higher expression of DNMT3a (Fig. 8A) may have contribution to the
398 genomic hyper-methylation of HFD oocytes because the primary function
399 of DNMT3a is *de novo* DNA methylations. The *de novo* methylation
400 function of DNMT1 is usually prevented by *Stella* (also known as *Dppa3*
401 or *PGC7*) in oocytes (*34*). Nevertheless, maternal obesity significantly
402 reduces the expression of *Stella* in oocytes (*3*), which indicates that
403 DNMT1 may also have contribution to the hyper-methylation of HFD
404 oocytes. We found that the localization of DNMT1 in HFD oocyte nucleus
405 was significantly increased which could be reduced by PKA antagonist
406 H89 2HCL treatment (n≥24 Fig. 8J, K). These results suggest that
407 increased DNMTs induced by maternal obesity has contributions to the
408 hyper-methylation of oocytes.

409 **Discussion**

410 Maternal obesity has negative effects on oocyte quality and offspring
411 health, but the mechanisms are not well elucidated. In the present study,
412 we found that maternal obesity induced hyper-methylation in oocytes, and
413 the abnormal methylation, at least partly, is transmitted to F2 oocytes in
414 females, which may be associated with the occurrence and inheritance of
415 metabolic disorders. Maternal obesity-induced metabolic changes may be

416 the cause of DNA hyper-methylation, anddecreased melatonin is involved
417 in regulating the hyper-methylation of HFD oocytes via increasing the
418 expression of DNMTs mediated by cAMP/PKA/CREB pathway.
419 Transgenerational epigenetic inheritance is common in plants, but related
420 investigation in mammals is hindered by epigenetic reprogramming events
421 during gametogenesis and early embryo development (*35, 36*). In
422 mammals, isogenic agouti viable yellow (A^{vy}) and axin-fused ($Axin^{Fu}$) mice,
423 whose phenotype is regulated by the DNA methylation level of *Iap* (intra-
424 cisternal A particle long terminal repeat) respectively located at the
425 upstream and in intron 6, are solid evidence confirming the
426 transgenerational inheritance of epigenetic modifications (*37, 38*).
427 Nevertheless, epigenetic modifications can be affected by environmental
428 factors such as metabolic diseases and diets. The intergenerational
429 inheritance of phenotype and epigenetic changes induced by maternal
430 environmental factors is confirmed by previous studies (*5, 39*), but there
431 are still many debates about the transgenerational inheritance of epigenetic
432 changes induced by environment. Rats from stressed mother are more
433 likely to be stressed, and this can be transmitted across generations, but this
434 transgenerational inheritance is not mediated by gametes (*40*). Females
435 cannot mediate the transgenerational inheritance of hyper-methylation
436 induced by diet in A^{vy} mice (*41*), but another study reported that if A^{vy} allele
437 is from father, the hyper-methylation induced by diet during pregnancy can

438 be retained in germ cells (*42*). Anway et al. report that the abnormal
439 spermatogenesis induced by exposure of vinclozolin during pregnancy can
440 be transmitted across four generations via sperm (*43*). We previously
441 reported that maternal obesity disturbed DNA methylation status of
442 imprinted genes in oocytes (*5*), but the transgenerational inheritance was
443 not observed. We also demonstrate that disturbed methylation in oocytes
444 induced by undernourishment in utero could be inherited, at least partly, by
445 F2 oocytes via females (*44*). Recently, Takahashi *et al.* edited DNA
446 methylation of promoter-associated CGIs, and found that the edited DNA
447 methylation, associated with disturbed metabolism, was stably inherited by
448 multiple generations (*45*). In the present study, we find that maternal
449 obesity induces genomic hyper-methylation in oocytes, and a part of the
450 abnormal methylation transmits to F2 via female gametes. Meanwhile, the
451 transmission of metabolic disorders is also observed across two
452 generations. These suggest that the transgenerational inheritance of
453 abnormal methylation induced by maternal obesity, at least partly, can be
454 mediated by oocytes, which may be a reason for the inheritance of
455 metabolic disorders.
456 During methylation process, the methyl group is donated by SAM which
457 is generated from homocysteine, 5-methyltetrahydrofolate (5mTHF), and
458 methionine. 5mTHF is an intermediate of one-carbon metabolism (*46*). It's
459 demonstrated that one-carbon units such as folate and vitamin B12 are

460 crucial for the establishment of methylation (*46*). Disturbed glucose and
461 lipid metabolism also has negative influence on DNA methylation (*47*).
462 These indicate that abnormal metabolism induced by maternal obesity (*48*)
463 may play a key role in the genomic hyper-methylation in oocytes. In the
464 present study, we find that the metabolomics of serum in HFD mice is
465 distinguishable with that in the CD control. Although the concentrations of
466 vitamin B6 and methionine are higher in HFD serum, it may be not an
467 important reason for the genomic hyper-methylation in oocytes because the
468 concentrations of SAM, SAH, and HCY in livers and oocytes are similar
469 between CD and HFD mice. In humans, obesity reduces the melatonin
470 level in circulation (*19, 20*). In the present study, we also find that maternal
471 obesity induced by high-fat diet reduces the concentration of melatonin in
472 serum. Melatonin not only can decrease body weight, but also regulates
473 DNA methylation of somatic cells and germ cells (*22, 26*). Nevertheless,
474 the molecular mechanism of melatonin regulating DNA methylation in
475 oocytes is still covered. Melatonin has two receptors, MT1 and MT2, both
476 of which have been identified in oocytes (*27*). Melatonin receptors couple
477 with inhibitor G-protein and can regulate gene expression via
478 cAMP/PKA/CREB pathway (*29*). CREM and cAMP mediate DNA
479 methylation in somatic cells by regulating the expression of *DNMT3a* (*30,*
480 *31*). In neurons, CREB interacts with promoter of *DNMT3a* to regulate its
481 expression and DNA methylation (*32*). In the present study, we find that

482 melatonin, mediated by cAMP/PKA/CREB pathway, regulates
483 methylation in oocytes by increasing the expression of DNMT1 and
484 DNMT3a. Similar results are also observed in HFD oocytes, and the hyper-
485 methylation of HFD oocytes can be reduced by exogenous melatonin and
486 PKA inhibitor. These suggest that decreased melatonin level is involved in
487 regulating the genomic hyper-methylation of HFD oocytes via increasing
488 the expression of DNMTs, mediated by cAMP/PKA/CREB pathway.
489 During follicular development, re-methylation in oocytes is mainly
490 catalyzed by DNMT3a and DNMT3l (*49*). DNMT1 is usually responsible
491 for DNA methylation maintain, but DNMT1 also contributes to CG
492 methylation in oocytes (*50*). In normal oocyte developing process,
493 DNMT1 is mainly prevented inthe nucleus by *Stella*. While *Stella* level is
494 reduced, *Uhrf1* (Ubiquitin-like containing PHD Ring Finger 1) moves to
495 the nucleus from cytoplasm and recruits DNMT1 to chromatin, resulting
496 in hyper-methylation (*33*). Maternal obesity significantly deceases the
497 expression of *Stella* in oocytes (*3*). We find that the expression of DNMT1
498 and its localization at chromatin in oocytes are increased by maternal
499 obesity. These suggest that reduced *Stella* in HFD oocytes may recruit
500 more DNMT1 into chromatin resulting in hyper-methylation.
501 In summary, we find that maternal obesity induces genomic hyper-
502 methylation in oocytes and at least a part of the altered methylation can be
503 transmitted to F2 oocytes, which may be a reason for the inheritance of

504 metabolic disorders. Furthermore, reduced melatonin in HFD mice is
505 involved in regulating the genomic hyper-methylation of oocytes via
506 increasing the expression of DNMTs, and this process is mediated by
507 cAMP/PKA/CREB pathway. However, there are some limitations about
508 the present study: there is no enough evidence to confirm the role of altered
509 DNA methylation in metabolic disorders in offspring of obese mothers, the
510 molecular mechanisms by which DNA methylation escapes
511 reprogramming in oogenesis is not elucidated. There are may be other
512 mechanisms involving in regulating genomic hyper-methylation in HFD
513 oocytes. Therefore, more studies are required in the short future.

514 **Materials and methods**

515 **Mice**

516 C57BL/6 mice were purchased from Jinan Pengyue Company (Jinan,
517 China). Mice were housed in the controlled room with 12h light and 12h
518 dark cycle, and at 23-25 ℃. The Animal Ethic Committee of Qingdao
519 Agricultural University supported all procedures (QAU201900326).

520 For obesity model, female C57BL/6 mice at the age of 4 weeks were
521 randomly divided into two groups fed with high-fat diet (HFD, Research
522 Diets, D12492, USA) and normal diet (CD) for 12 weeks, respectively. We
523 examined the body weight every week.

524 Offspring were produced as the schedule Fig.1J. For F1 offspring, female
525 HFD and CD mice were mated with normal adult male C57BL/6 mice,

526 respectively, and the offspring was marked as HF1 and CF1. To avoid the
527 effects of males on methylation, the same males were used to produce F2:
528 female HF1 and CF1 mating with normal males, marked as HF2 and CF2.

529 **Immunofluorescence**

530 Briefly, oocytes were fixed with 4% PFA (paraformaldehyde),
531 permeabilized with 0.5% TritonX-100, and blocked with 1% BSA (bovine
532 serum albumin). After that, oocytes were incubated with primary
533 antibodies overnight. The secondary antibodies were stained for 1h at room
534 temperature. Fluorescence signal was examined using a laser scanning
535 confocal microscope (Leica SP5, Germany). Relative fluorescence
536 intensity was examined using Image J.

537 **Antibodies**

538 Primary antibodies used in the present study included anti-5mC antibody
539 (Abcam, ab73938), anti-5hmC antibody (Abcam, ab214728), anti-pCREB
540 antibody (Cell Signaling Technology, 9198S), anti-DNMT3a antibody
541 (Active motif, 61478), and anti-DNMT1 antibody (Active motif, 39204).

542 **Single cell whole genome bisulfite sequencing (scWGBS) and analysis**

543 Metaphase II (MII) oocytes were collected from the oviduct. For each
544 sample, 100 oocytes from at least 10 mice were pooled together and
545 transferred to lysis buffer. Genomic DNA was fragmented and the end was
546 repaired. Then, fragmentations were ligated with adapter. Bisulfite
547 treatment was performed using EZ DNA Methylation-Direct (Zymo

548 Research). Lambda DNA was used as control. After that, the sequencing
549 library was established and sequenced using Illumina HiSeq/NovaSeq
550 (Novogene, China). Raw data quality was evaluated using FastQC, and low
551 quality data and adapter was trimmed using fastp. Clean data was
552 compared to the reference genome mm10. Methylated C sites calling were
553 performed using Bismark. Differentially methylated regions (DMRs) were
554 identified using DSS-single. The enrichment of genes in KEGG pathway
555 was carried out using the online tool KOBAS.

556 **qPCR**

557 Total RNA was extracted from oocytes or tissues using RNAprep Pure
558 Micro Kit (Tiangen, DP420) or RNA Easy Fast Kit (Tiangen, DP451).
559 cDNA was synthesized using Hifair III 1st Strand cDNA Synthesis Kit
560 (Yeasen, China). cDNA was used as templates to examined the relative
561 expression of genes. Housekeeping genes *Ppia* and *Gapdh* were used as
562 reference. Relative expression was calculated as $2^{-\Delta\Delta Ct}$.

563 **Bisulfite sequencing (BS)**

564 Each sample includes 5 oocytes and at least 20 samples were used for each
565 DMR. Samples were treated as previous study (*5*). Briefly, samples were
566 treated with lysis buffer and 0.3M NaOH, respectively. After that, samples
567 were embedded with 2% low melting point agarose (Sigma), which was
568 treated with fresh bisulfite solution (2.5 M sodium metabisulfite, Merck;
569 125 mM hydroquinone, Sigma; pH 5) for 4h. Treated DNA was used as

570 template to amplify the target fragment using nest-PCR. PCR products
571 were cloned to T-vector and sequenced. Methylation status was analyzed
572 using BiqAnalyzer, which can remove the low converted rate (<97%) and
573 possible repeat sequences. At least 10 available clones was used for each
574 DMR.

575 **Glucose and insulin tolerance**

576 Glucose and insulin tolerance (GTT and ITT) were examined as previously
577 reported (*7*). Briefly, mice were treated with glucose at 2g/kg body weight
578 or insulin (Actrapid®, Novo Nordisk) at 10 IU/kg body weight after 16h
579 or 4h fasting, respectively. After that, blood glucose was measured by tail
580 blood at 0, 30, 60, 90, and 120 min, respectively.

581 **ELISA**

582 Concentrations of cAMP, SAM, SAH, and HCY were examined using
583 ELISA kits (Jinma Biotechnology Co. LTD, Shanghai, China) according to
584 the handbook. Standard curve was produced using four-parameters
585 logistics.

586 **Non-target metabolomics in serum**

587 Metabolites in serum were examined using LC-MS/MS (BGI, Wuhan,
588 China). Raw date was treated with Compound Discoverer 3.1 (Thermo
589 Fisher Scientific, USA). After that, preprocessing of the exported data was
590 performed using metaX. Metabolites were identified according to the
591 databases of BMDB (BGI), mzCloud and ChemSpider (HMDB, KEGG,

592 LipidMaps). Identified metabolites were annotated according to KEGG
593 and HMDB. Differential metabolites were scanned using PCA and PLS-
594 DA combined with Fold-change and Student's t test.

595 **Chemicals**

596 Inhibitors used in the present study include luzindole (Sigma), SQ22536
597 (Selleck), forskolin (Selleck), H89 2HCL (Selleck), and azacitidine
598 (Selleck). 8-Bromo-cAMP was purchased from Selleck. Melatonin (Sigma)
599 was injected by tail vein for 14 days. The treatments of the other chemicals
600 were performed by intraperitoneal injection for 14 days. The control group
601 was injected with relative solutions.

602 **CUT & Tag and sequencing**

603 For each sample, 500 oocytes were pooled together for this experiment,
604 and two replicates were performed. Library was established using
605 Hyperactive® Universal CUT&Tag Assay Kit (Vazyme, China) according
606 to the manufacturer's instruction. Briefly, oocytes washed with washing
607 buffer and transferred into tubes with ConA Beads Pro for 10min in room
608 temperature. Putting tubes on magnetic rack for 2min, and then discarded
609 the supernatant. After that, added 50 μl precooled antibody buffer and
610 primary antibody overnight at 4 ℃. Then, tubes were put on magnetic rack
611 for 2 min, discarded supernatant, and added 50 μl Dig-wash buffer with
612 secondary antibody (1:100) into tubes incubated at room temperature for
613 60 min. Samples were washed three times, and then incubated with pA/G-

614 Tnp pro for 1h at room temperature. After washing, 50 μl TTBL was added
615 into samples and incubated at 37 ℃ for 1h. Then, added 2 μl 10% SDS
616 and DNA Spike-in into samples incubated at 55 ℃ for 10 min.
617 Supernatant was transferred into a new tube after putting on magnetic rack
618 for 2 min. 25 μl DNA Extract Beads Pro was added into supernatant
619 incubated 20 min at room temperature, and then washed two times using
620 B&W buffer. After that, DNA Extract Beads Pro was re-suspended in 15
621 μl ddH_2O, and amplified at 60 ℃ for 20 cycles. Library quality was
622 examined using Qubit, AATI, and QPCR, and then sequenced using
623 NovaSeq 6000 (Novogene, China). Adaptor and low-quality reads were
624 removed from raw data, and clean data was used for further analysis. Reads
625 were mapped to mouse reference genome mm39 using Bowtie2. Peak
626 calling was performed using MACS2 at q-value <0.05. Then, peak was
627 annotated into relative gene regions.

628 **Statistical analysis**

629 Average data are presented as mean ± SE (standard error), and the
630 statistical difference was calculated using two-tail independent-samples t
631 test. Methylation level was presented as percentage, and the statistical
632 difference was calculated using Chi-square test. If p value < 0.05, the
633 statistical difference was considered to be significant.

634 **Acknowledgement**

635 This work was supported by the National Natural Science Foundation of

China (31872312), National R&D Program of China (2022YFC2703500), the Breeding Plan of Shandong Provincial Qingchuang Research Team (Innovation Team of Farm Animal Cloning 012–1622001), and the Doctor Foundation of Qingdao Agricultural University (6631116008).

Conflicts of interest statement

There are no conflicts of interest to declare.

Data availability

The raw data of sequencing is submitted to the database BGI Sub with No. CRA011654.

1. X. Chen, Z. Xiao, Y. Cai, L. Huang, C. Chen, Hypothalamic mechanisms of obesity-associated disturbance of hypothalamic-pituitary-ovarian axis. *Trends Endocrinol Metab* **33**, 206-217 (2022).
2. D. E. Broughton, K. H. Moley, Obesity and female infertility: potential mediators of obesity's impact. *Fertil Steril* **107**, 840-847 (2017).
3. L. Han *et al.*, Embryonic defects induced by maternal obesity in mice derive from Stella insufficiency in oocytes. *Nat Genet* **50**, 432-442 (2018).
4. K. M. Godfrey *et al.*, Influence of maternal obesity on the long-term health of offspring. *Lancet Diabetes Endocrinol* **5**, 53-64 (2017).
5. Z. J. Ge *et al.*, DNA methylation in oocytes and liver of female mice and their offspring: effects of high-fat-diet-induced obesity. *Environ Health Perspect* **122**, 159-164 (2014).
6. D. Amrom, S. S. Schwartz, Maternal Metabolic Health, Lifestyle, and Environment - Understanding How Epigenetics Drives Future Offspring Health. *Curr Diabetes Rev*, (2022).
7. S. B. Tang *et al.*, Inheritance of perturbed methylation and metabolism caused by uterine malnutrition via oocytes. *BMC Biol* **21**, 43 (2023).
8. J. A. Jacobsson *et al.*, Genetic variants near the MGAT1 gene are associated with body weight, BMI and fatty acid metabolism among adults and children. *Int J Obes (Lond)* **36**, 119-129 (2012).
9. A. Johansson *et al.*, Linkage and genome-wide association analysis of obesity-related phenotypes: association of weight with the MGAT1 gene. *Obesity (Silver Spring)* **18**, 803-808 (2010).
10. V. Bartakova *et al.*, Dysfunctional protection against advanced glycation due to thiamine metabolism abnormalities in gestational diabetes. *Glycoconj J* **33**, 591-598 (2016).
11. H. Kang *et al.*, PARIS reprograms glucose metabolism by HIF-1alpha induction in dopaminergic neurodegeneration. *Biochem Biophys Res Commun* **495**, 2498-2504 (2018).

12. V. L. Hood, R. Berger, R. Freedman, A. J. Law, Transcription of PIK3CD in human brain and schizophrenia: regulation by proinflammatory cytokines. *Hum Mol Genet* **28**, 3188-3198 (2019).
13. M. Wojcik *et al.*, The association of leukocyte phosphatidylinositol 3-kinase delta overexpression with gestational diabetes mellitus (GDM). *Endokrynol Pol* **65**, 17-24 (2014).
14. L. Shou, F. Pan, S. Chin, Pancreatic hormones and hepatic methionine adenosyltransferase in the rat. *Proc Soc Exp Biol Med* **131**, 1012-1018 (1969).
15. P. Lyon, V. Strippoli, B. Fang, L. Cimmino, B Vitamins and One-Carbon Metabolism: Implications in Human Health and Disease. *Nutrients* **12**, (2020).
16. D. H. Chen, K. T. Wu, C. J. Hung, M. Hsieh, C. Li, Effects of adenosine dialdehyde treatment on in vitro and in vivo stable protein methylation in HeLa cells. *J Biochem* **136**, 371-376 (2004).
17. J. A. Vaccaro, S. A. Naser, The Role of Methyl Donors of the Methionine Cycle in Gastrointestinal Infection and Inflammation. *Healthcare (Basel)* **10**, (2021).
18. R. A. Waterland, Assessing the effects of high methionine intake on DNA methylation. *J Nutr* **136**, 1706S-1710S (2006).
19. L. Virto *et al.*, Melatonin expression in periodontitis and obesity: An experimental in-vivo investigation. *J Periodontal Res* **53**, 825-831 (2018).
20. J. Overberg *et al.*, Interactions between nocturnal melatonin secretion, metabolism, and sleeping behavior in adolescents with obesity. *Int J Obes (Lond)* **46**, 1051-1058 (2022).
21. Q. Guan, Z. Wang, J. Cao, Y. Dong, Y. Chen, Mechanisms of Melatonin in Obesity: A Review. *Int J Mol Sci* **23**, (2021).
22. A. Davoodvandi, B. Nikfar, R. J. Reiter, Z. Asemi, Melatonin and cancer suppression: insights into its effects on DNA methylation. *Cell Mol Biol Lett* **27**, 73 (2022).
23. J. Qu *et al.*, Melatonin Enhances the Development of Porcine Cloned Embryos by Improving DNA Methylation Reprogramming. *Cell Reprogram* **22**, 156-166 (2020).
24. S. Saeedabadi, A. H. Abazari-Kia, H. Rajabi, K. Parivar, M. Salehi, Melatonin Improves The Developmental Competence of Goat Oocytes. *Int J Fertil Steril* **12**, 157-163 (2018).
25. P. Xiao *et al.*, Melatonin alleviates the deterioration of oocytes from mice subjected to repeated superovulation. *J Cell Physiol* **234**, 13413-13422 (2019).
26. M. Lan *et al.*, Melatonin protects against defects induced by deoxynivalenol during mouse oocyte maturation. *J Pineal Res* **65**, e12477 (2018).
27. J. Wang *et al.*, Melatonin Alleviates the Suppressive Effect of Hypoxanthine on Oocyte Nuclear Maturation and Restores Meiosis via the Melatonin Receptor 1 (MT1)-Mediated Pathway. *Front Cell Dev Biol* **9**, 648148 (2021).
28. J. X. Jin *et al.*, Melatonin Regulates Lipid Metabolism in Porcine Cumulus-Oocyte Complexes via the Melatonin Receptor 2. *Antioxidants (Basel)* **11**, (2022).
29. P. Wongprayoon, P. Govitrapong, Melatonin Receptor as a Drug Target for Neuroprotection. *Curr Mol Pharmacol* **14**, 150-164 (2021).
30. X. Fang *et al.*, cAMP induces hypertrophy and alters DNA methylation in HL-1 cardiomyocytes. *Am J Physiol Cell Physiol* **309**, C425-436 (2015).
31. C. M. Hedrich *et al.*, cAMP responsive element modulator (CREM) alpha mediates chromatin remodeling of CD8 during the generation of CD3+ CD4- CD8- T cells. *J Biol Chem* **289**, 2361-2370 (2014).

715 32. Y. Yang *et al.*, CREB Participates in Paclitaxel-Induced Neuropathic Pain Genesis Through
716 Transcriptional Activation of Dnmt3a in Primary Sensory Neurons. *Neurotherapeutics* **18**,
717 586-600 (2021).
718 33. Y. Li *et al.*, Stella safeguards the oocyte methylome by preventing de novo methylation
719 mediated by DNMT1. *Nature* **564**, 136-140 (2018).
720 34. M. Bostick *et al.*, UHRF1 plays a role in maintaining DNA methylation in mammalian cells.
721 *Science* **317**, 1760-1764 (2007).
722 35. R. J. Schmitz, J. R. Ecker, Epigenetic and epigenomic variation in Arabidopsis thaliana.
723 *Trends Plant Sci* **17**, 149-154 (2012).
724 36. M. J. Xavier, S. D. Roman, R. J. Aitken, B. Nixon, Transgenerational inheritance: how impacts
725 to the epigenetic and genetic information of parents affect offspring health. *Hum Reprod*
726 *Update* **25**, 518-540 (2019).
727 37. V. K. Rakyan, M. E. Blewitt, R. Druker, J. I. Preis, E. Whitelaw, Metastable epialleles in
728 mammals. *Trends Genet* **18**, 348-351 (2002).
729 38. H. D. Morgan, H. G. Sutherland, D. I. Martin, E. Whitelaw, Epigenetic inheritance at the
730 agouti locus in the mouse. *Nat Genet* **23**, 314-318 (1999).
731 39. B. Chen *et al.*, Maternal inheritance of glucose intolerance via oocyte TET3 insufficiency.
732 *Nature* **605**, 761-766 (2022).
733 40. I. C. Weaver *et al.*, Epigenetic programming by maternal behavior. *Nat Neurosci* **7**, 847-
734 854 (2004).
735 41. R. A. Waterland, M. Travisano, K. G. Tahiliani, Diet-induced hypermethylation at agouti
736 viable yellow is not inherited transgenerationally through the female. *The FASEB Journal*
737 **21**, 3380-3385 (2007).
738 42. J. E. Cropley, C. M. Suter, K. B. Beckman, D. I. K. Martin, Germ-line epigenetic modification
739 of the murine Avy allele by nutritional supplementation. *Proceedings of the National*
740 *Academy of Sciences* **103**, 17308-17312 (2006).
741 43. M. D. Anway, A. S. Cupp, M. Uzumcu, M. K. Skinner, Epigenetic Transgenerational Actions
742 of Endocrine Disruptors and Male Fertility. *Science* **308**, 1466-1469 (2005).
743 44. S.-B. Tang *et al.*, Inheritance of perturbed methylation and metabolism caused by uterine
744 malnutrition via oocytes. *BMC Biology* **21**, (2023).
745 45. Y. Takahashi *et al.*, Transgenerational inheritance of acquired epigenetic signatures at CpG
746 islands in mice. *Cell* **186**, 715-731 e719 (2023).
747 46. S. J. Mentch, J. W. Locasale, One-carbon metabolism and epigenetics: understanding the
748 specificity. *Ann N Y Acad Sci* **1363**, 91-98 (2016).
749 47. M. Keller *et al.*, Global DNA methylation levels in human adipose tissue are related to fat
750 distribution and glucose homeostasis. *Diabetologia* **57**, 2374-2383 (2014).
751 48. J. C. King, Maternal obesity, metabolism, and pregnancy outcomes. *Annu Rev Nutr* **26**,
752 271-291 (2006).
753 49. K. Kibe *et al.*, The DNMT3A PWWP domain is essential for the normal DNA methylation
754 landscape in mouse somatic cells and oocytes. *PLoS Genet* **17**, e1009570 (2021).
755 50. K. Shirane *et al.*, Mouse oocyte methylomes at base resolution reveal genome-wide
756 accumulation of non-CpG methylation and role of DNA methyltransferases. *PLoS Genet*
757 **9**, e1003439 (2013).

758 **Figure legend**

759 **Figure1 Maternal obesity alters DNA methylation of oocytes.**

760 (A) Methylation level of 5mC and 5hmC in oocytes. 5mC, 5-
761 methylcytosine; 5hmC, 5-hydroxymethylcytosine; DAPI, chromatin.

762 (B, C) Relative fluorescence intensity of 5mC and 5hmC in GV oocytes.

763 (D) Genomic methylation level of MII oocytes examined by single-cell
764 whole genome bisulfite sequencing. Control group (CD) has two replicates,
765 and obesity group (HFD) has three replicates.

766 (E) Average genomic CG methylation level in MII oocytes. CD, control
767 group; HFD, obesity group; ** means p value < 0.01.

768 (F) CG methylation levels at different regions in MII oocytes. CGI, CpG
769 Island; utr5, 5' untranslated region; utr3, 3' untranslated region; repeat,
770 repeat sequence.

771 (G) Total differentially methylated regions (DMRs) in oocytes of control
772 and obesity groups . hyper-DMRs, hypermethylated DMRs; hypo-DMRs,
773 hypomethylated DMRs.

774 (H) Distribution of DMRs on chromosomes in MII oocytes. Outside-to-in:
775 chromosome, hyper-DMRs, TE (transcription end region), and gene, hypo-
776 DMRs.

777 (I) Enrichment of genes with DMRs at the promoter regions in KEGG
778 pathways, and the top 20 pathways were presented.

779 (J) Schedule of breeding. Female C57BL/6 were fed with normal (CD) or
780 high-fat diet (HFD) for 12 weeks marked as F0. F1 was produced by F0

781 mating with normal males, respectively, and marked as CF1 and HF1; F2
782 was produced by female F1 mating with normal males and marked as CF2
783 and HF2, respectively.

784 **Figure 2 Transgenerational inheritance of metabolic disorders and**
785 **altered DNA methylation.**

786 (A-C) Glucose tolerance (GTT) and insulin tolerance ITT) were tested
787 for female F0, F1, and F2, respectively. * $p<0.05$; ** $p<0.01$.

788 (D-F) DMR methylation at the promoter regions of *Bhlha15*, *Mgat1*, *Taok3*,
789 *Tkt*, and *Pid3cd* in F0, F1, and F2 oocytes were respectively examined
790 using bisulfite sequencing. At least 10 available clones from 80-100
791 oocytes were used to calculate the methylation level. White circle,
792 unmethylated CG; black circle, methylated CG. * $p<0.05$; ** $p<0.01$.

793 (G) Inheritance of altered methylation in different generations was
794 analyzed. * $p<0.05$; ** $p<0.01$.

795 **Figure 3 Maternal obesity alters metabolomics of serum.**

796 (A) Principal component analysis in CD and HFD mice.

797 (B) Differential metabolites in HFD serum compared to CD group. Red
798 circle, up regulated metabolites; blue circle, down regulated metabolites.

799 (C) The enrichment of differential metabolites was analyzed using KEGG,
800 and the top 10 enrichment term was presented.

801 (D) Heat map of the top 20 differential metabolites in HFD serum.

802 (E-G) Comparison of the concentrations of pyridoxine, methionine, and

803 tyrosine between groups. * $p<0.05$; ** $p<0.01$; *** $p<0.001$.

804 (H-J) Concentrations of SAM, SAH and HCY in livers were examined by

805 ELISA. Ns, there is no statistical significance between groups.

806 (K) Concentration of SAM in oocytes was analyzed using ELISA. **

807 $p<0.01$.

808 (L) Relative concentration of melatonin in serum. *** $p<0.001$.

809 (M) Genomic DNA methylation in oocytes was examined using

810 immunofluorescence. CD, control group; HFD, obesity group;

811 HFD+melatonin, obese mice were treated with exogenous melatonin for

812 14 days.

813 (N) Relative fluorescence intensity of 5mC was examined using Image J.

814 * $p<0.05$; *** $p<0.001$.

815 **Figure 4 Melatonin regulates DNA methylation in oocytes.**

816 (A) Schedule of possible pathway of melatonin regulating DNA

817 methylation in oocytes. According to previous studies, we predicted that

818 melatonin might regulate DNA methylation in oocytes via

819 cAMP/PKA/CREB pathway.

820 (B) Effects of melatonin and its inhibitor luzindole on oocyte methylation

821 were examined using immunofluorescence.

822 (C, D) The relative fluorescence intensities of 5mC and 5hmC were

823 analyzed using Image J. * $p<0.05$; *** $p<0.001$.

824 (E) The effects of melatonin and its inhibitor luzindole on the expression

825 of adenylate cyclase (ADCYs) in oocytes were examined by qPCR. *
826 $p<0.05$; ** $p<0.01$.
827 (F) Concentration of cAMP in oocytes was examined by ELISA. * $p<0.05$;
828 ** $p<0.01$.
829 **Figure 5 Role of cAMP in DNA methylation in oocytes.**
830 (A) Female mice were respectively treated with ADCYs inhibitor SQ22536
831 or activator forskolin. Oocyte methylation was examined using
832 immunofluorescence.
833 (B) The relative intensity of fluorescence in oocytes was analyzed using
834 Image J. ** $p<0.01$; *** $p<0.001$.
835 (C) cAMP concentration in oocytes was examined using ELISA. * $p<0.05$;
836 ** $p<0.01$.
837 (D) Female mice were treated with cAMP analogue 8-Bromo-cAMP, and
838 oocyte methylation was examined using immunofluorescence. The relative
839 fluorescence intensity of 5mC was analyzed using Image J (E). ** $p<0.01$.
840 (F, G) Female mice were treated with PKA (protein kinase A) antagonist H
841 89 2HCL, and then oocyte methylation was examined using
842 immunofluorescence. The relative fluorescence intensity of 5mC was
843 analyzed using Image J (G). * $p<0.05$.
844 **Figure 6 Effects of cAMP on CREB1.**
845 (A) The mRNA expression of cAMP-response element binding (CREB)
846 proteins in oocytes was examined by qPCR. * $p<0.05$.

847 (B and C) Phosphorylated CREB1 (pCREB1) in oocytes was examined
848 using immunofluorescence, and the relative fluorescence intensity of
849 pCREB1 was examined by Image J (C). * $p<0.05$; ** $p<0.01$; *** $p<0.001$.
850 (D and E) After treatment of cAMP analogue 8-Bromo-cAMP, pCREB1 in
851 oocytes was examined using immunofluorescence. The relative
852 fluorescence intensity was analyzed using Image J (E). *** $p<0.001$.

853 **Figure 7 Role of melatonin/cAMP/PKA pathway in the expression of**
854 **DNMTs.**

855 (A) The expressions of DNMT1, DNMT3a and DNMT3l in oocytes were
856 examined using qPCR after the treatment with SQ22536 and forskolin. *
857 $p<0.05$.
858 (B) Relative expressions of DNMT1, DNMT3a and DNMT3l in oocytes
859 were examined using qPCR after the treatment with luzindole and
860 melatonin. * $p<0.05$.
861 (C) After 8-Bromo-cAMP treatment, the relative expression of DNMT3a
862 in oocytes was examined using immunofluorescence and calculated by
863 Image J (D). ** $p<0.01$.
864 (E and F) PKA antagonist H 89 2HCL treatment significantly reduced the
865 level of DNMT3a in oocytes examined using immunofluorescence. **
866 $p<0.01$.
867 (G and H) DNMT1 localization in oocyte nucleus was examined using
868 immunofluorescence after 8-Bromo-cAMP treatment. *** $p<0.001$.

869 (I and J) The localization of DNMT1 in oocyte nucleus was reduced by the
870 treatment of PKA antagonist H 89 2HCL. ** $p<0.01$.

871 **Figure 8 Melatonin regulates DNMTs expression via**
872 **cAMP/PKA/CREB pathway in HFD oocytes.**

873 (A) Relative expression of DNMT1, DNMT3a, and DNMT3l in HFD
874 oocytes was examined using qPCR. * $p<0.05$; ** $p<0.01$.

875 (B) Concentration of cAMP in HFD oocytes was examined using ELISA.
876 ** $p<0.01$.

877 (C) Relative expressions CREB1 and CREM in HFD oocytes were tested
878 using qPCR. * $p<0.05$; ** $p<0.01$.

879 (D and E) The level of pCREB1 in oocytes was examined using
880 immunofluorescence, and the relative fluorescence intensity was
881 calculated by Image J (E). HFD, oocytes from obese mice; CD, oocytes
882 from control mice; HFD + melatonin, oocytes from obese mice treated with
883 exogenous melatonin. * $p<0.05$; *** $p<0.001$.

884 (F and G) PKA antagonist H89 2HCL treatment reduced the methylation
885 level of HFD oocytes. ** $p<0.01$; *** $p<0.001$.

886 (H and I) The level of pCREB1 in HFD oocytes was also decreased by the
887 treatment of PKA antagonist H89 2HCL. * $p<0.05$; ** $p<0.01$; ns, no
888 statistical significance between groups.

889 (J and K) PKA antagonist H89 2HCL treatment reduced the localization of
890 DNMT1 in HFD oocytes. ** $p<0.01$; *** $p<0.001$; ns, no statistical

891 significance between groups.

892

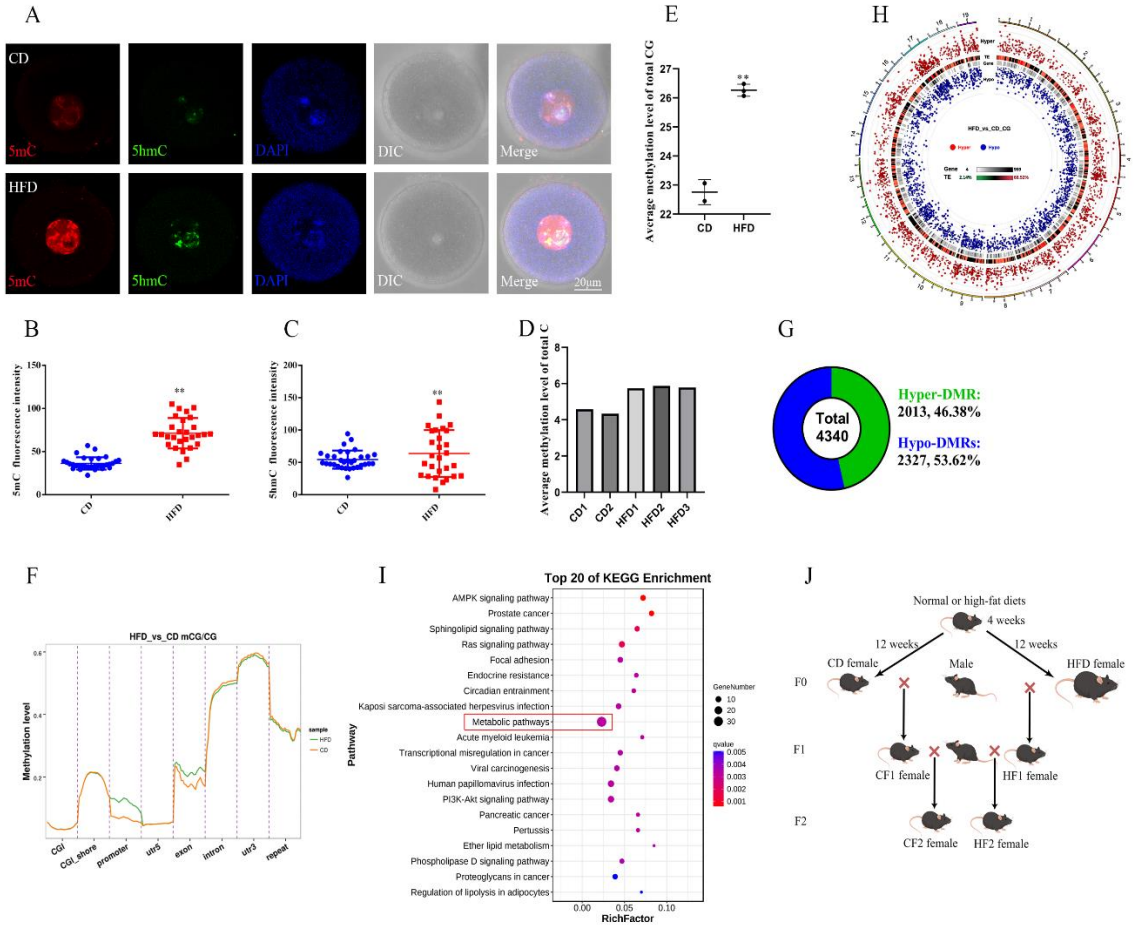

FiguresFigure1 Maternal obesity alters DNA methylation of oocytes.

(A) Methylation level of 5mC and 5hmC in oocytes. 5mC, 5-methylcytosine; 5hmC, 5-hydroxymethylcytosine; DAPI, chromatin.

(B, C) Relative fluorescence intensity of 5mC and 5hmC in GV oocytes.

(D) Genomic methylation level of MII oocytes examined by single-cell whole genome bisulfite sequencing. Control group (CD) has two replicates, and obesity group (HFD) has three replicates.

(E) Average genomic CG methylation level in MII oocytes. CD, control group; HFD, obesity group; ** means p value < 0.01.

(F) CG methylation levels at different regions in MII oocytes. CGI, CpG Island; utr5, 5’ untranslated region; utr3, 3’ untranslated region; repeat, repeat sequence.

(G) Total differentially methylated regions (DMRs) in oocytes of control and obesity groups . hyper-DMRs, hypermethylated DMRs; hypo-DMRs, and HF2, respectively.

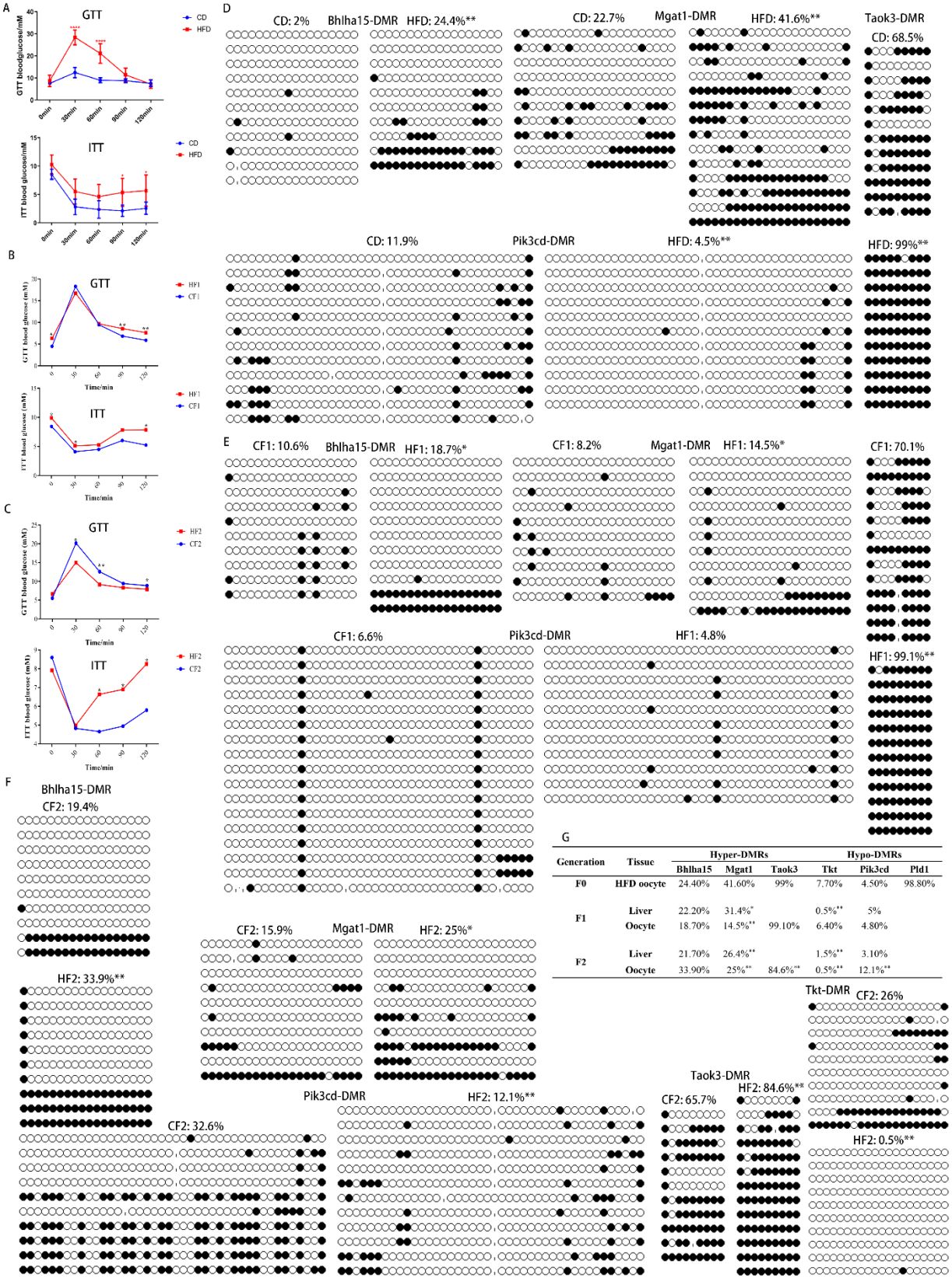

G

Generation	Tissue	Hyper-DMRs			Hypo-DMRs		
		Bhlha15	Mgat1	Taok3	Tkt	Pik3cd	Pld1
F0	HFD oocyte	24.40%	41.60%	99%	7.70%	4.50%	98.80%
F1	Liver	22.20%	31.4%*		0.5%**	5%	
	Oocyte	18.70%	14.5%**	99.10%	6.40%	4.80%	
F2	Liver	21.70%	26.4%**		1.5%**	3.10%	
	Oocyte	33.90%	25%**	84.6%**	0.5%**	12.1%**	

Figure 2 Transgenerational inheritance of metabolic disorders and altered DNA methylation.

(A-C) Glucose tolerance (GTT) and insulin tolerance ITT) were tested for female F0, F1, and F2, respectively. * $p<0.05$; ** $p<0.01$.

(D-F) DMR methylation at the promoter regions of *Bhlha15*, *Mgat1*, *Taok3*, *Tkt*, and *Pid3cd* in F0, F1, and F2 oocytes were respectively examined using bisulfite sequencing. At least 10 available clones from 80-100 oocytes were used to calculate the methylation level. White circle, unmethylated CG; black circle, methylated CG. * $p<0.05$; ** $p<0.01$.

(G) Inheritance of altered methylation in different generations was analyzed. * $p<0.05$; ** $p<0.01$.

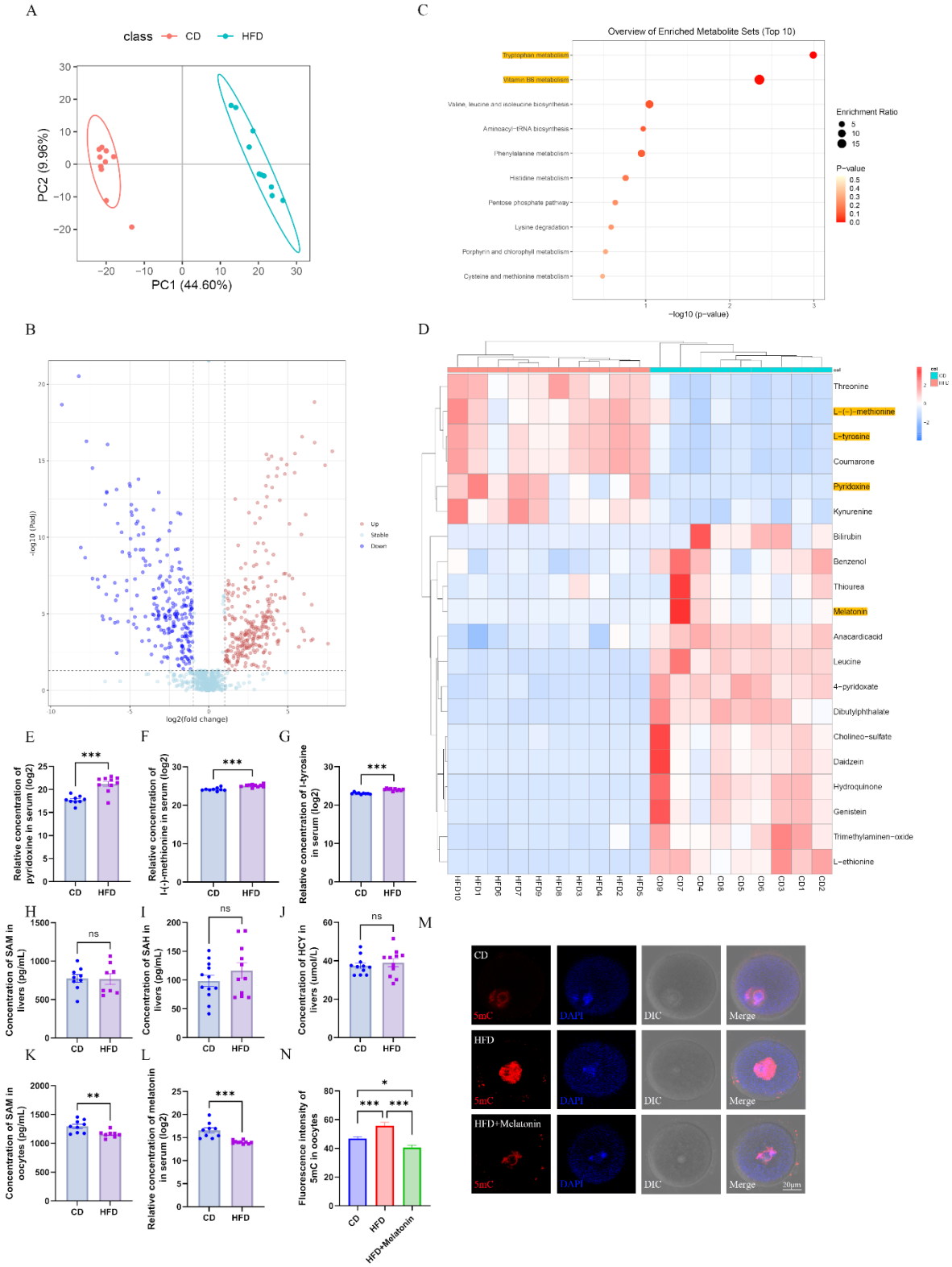

Figure 3 Maternal obesity alters metabolomics of serum.

(A) Principal component analysis in CD and HFD mice.

(B) Differential metabolites in HFD serum compared to CD group. Red

circle, up regulated metabolites; blue circle, down regulated metabolites.

(C) The enrichment of differential metabolites was analyzed using KEGG, and the top 10 enrichment term was presented.

(D) Heat map of the top 20 differential metabolites in HFD serum.

(E-G) Comparison of the concentrations of pyridoxine, methionine, and tyrosine between groups. * $p<0.05$; ** $p<0.01$; *** $p<0.001$.

(H-J) Concentrations of SAM, SAH and HCY in livers were examined by ELISA. Ns, there is no statistical significance between groups.

(K) Concentration of SAM in oocytes was analyzed using ELISA. ** $p<0.01$.

(L) Relative concentration of melatonin in serum. *** $p<0.001$.

(M) Genomic DNA methylation in oocytes was examined using immunofluorescence. CD, control group; HFD, obesity group; HFD+melatonin, obese mice were treated with exogenous melatonin for 14 days.

(N) Relative fluorescence intensity of 5mC was examined using Image J. * $p<0.05$; *** $p<0.001$.

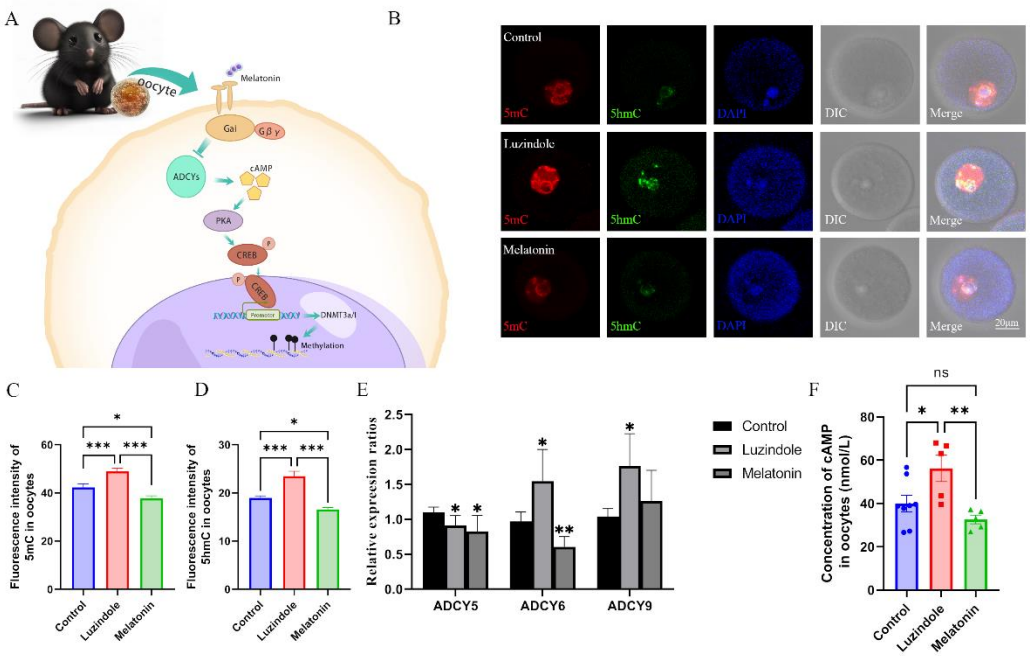

Figure 4 Melatonin regulates DNA methylation in oocytes.

(A) Schedule of possible pathway of melatonin regulating DNA methylation in oocytes. According to previous studies, we predicted that melatonin might regulate DNA methylation in oocytes via cAMP/PKA/CREB pathway.

(B) Effects of melatonin and its inhibitor luzindole on oocyte methylation were examined using immunofluorescence.

(C, D) The relative fluorescence intensities of 5mC and 5hmC were analyzed using Image J. * $p<0.05$; *** $p<0.001$.

(E) The effects of melatonin and its inhibitor luzindole on the expression of adenylate cyclase (ADCYs) in oocytes were examined by qPCR. * $p<0.05$; ** $p<0.01$.

(F) Concentration of cAMP in oocytes was examined by ELISA. * $p<0.05$; ** $p<0.01$.

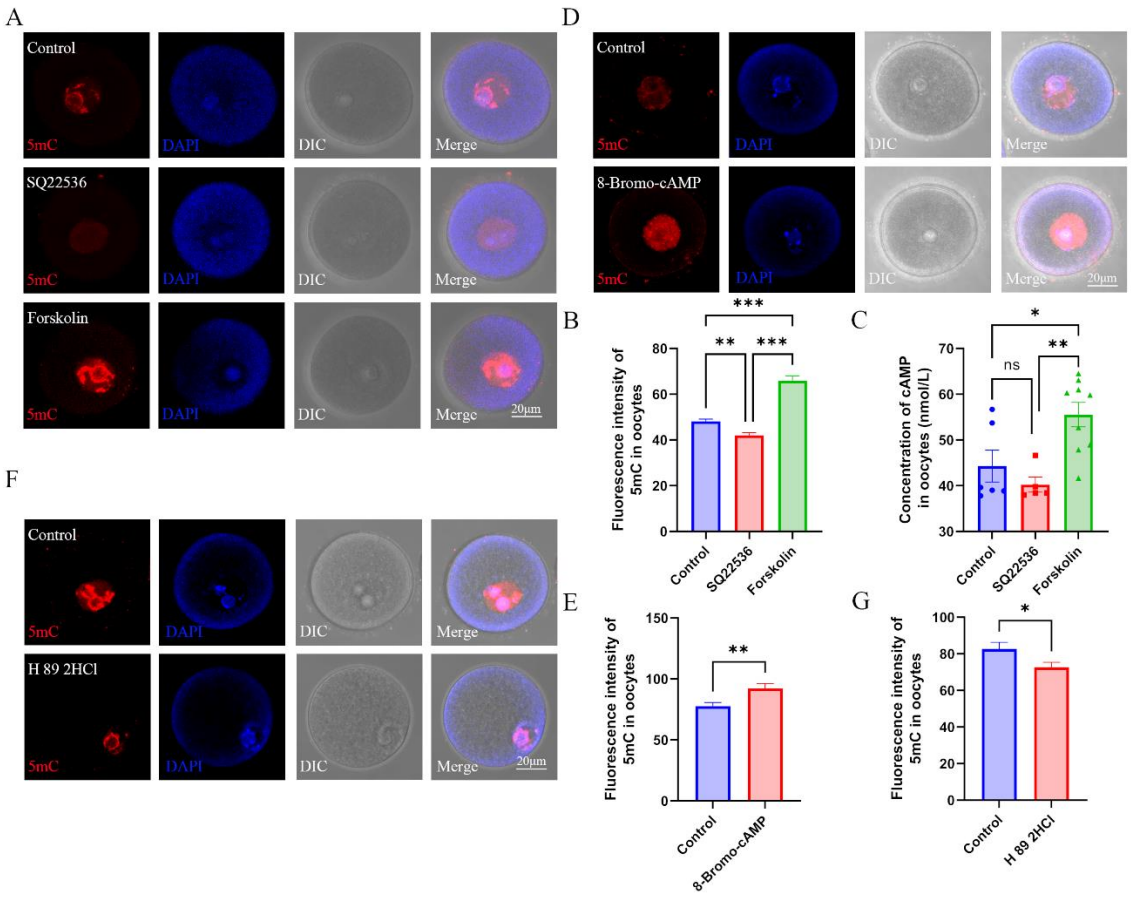

Figure 5 Role of cAMP in DNA methylation in oocytes.

(A) Female mice were respectively treated with ADCYs inhibitor SQ22536 or activator forskolin. Oocyte methylation was examined using immunofluorescence.

(B) The relative intensity of fluorescence in oocytes was analyzed using Image J. ** $p<0.01$; *** $p<0.001$.

(C) cAMP concentration in oocytes was examined using ELISA. * $p<0.05$; ** $p<0.01$.

(D) Female mice were treated with cAMP analogue 8-Bromo-cAMP, and oocyte methylation was examined using immunofluorescence. The relative fluorescence intensity of 5mC was analyzed using Image J (E). ** $p<0.01$.

(F, G) Female mice were treated with PKA (protein kinase A) antagonist H 89 2HCL, and then oocyte methylation was examined using immunofluorescence. The relative fluorescence intensity of 5mC was analyzed using Image J (G). * p<0.05.

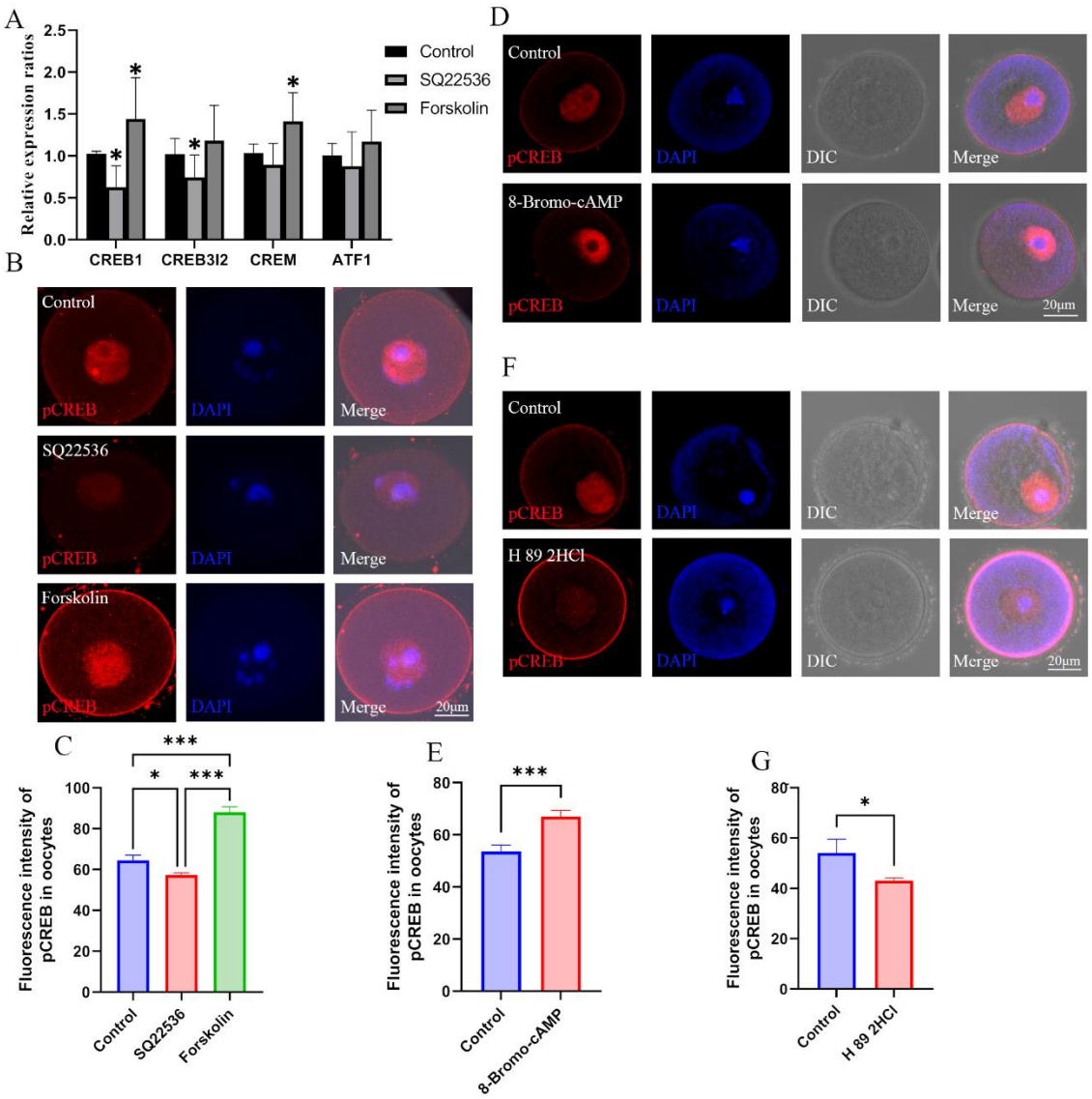

Figure 6 Effects of cAMP on CREB1.

(A) The mRNA expression of cAMP-response element binding (CREB) proteins in oocytes was examined by qPCR. * p<0.05.

(B and C) Phosphorylated CREB1 (pCREB1) in oocytes was examined

using immunofluorescence, and the relative fluorescence intensity of pCREB1 was examined by Image J (C). * p<0.05; ** p<0.01; *** p<0.001. (D and E) After treatment of cAMP analogue 8-Bromo-cAMP, pCREB1 in oocytes was examined using immunofluorescence. The relative fluorescence intensity was analyzed using Image J (E). *** p<0.001.

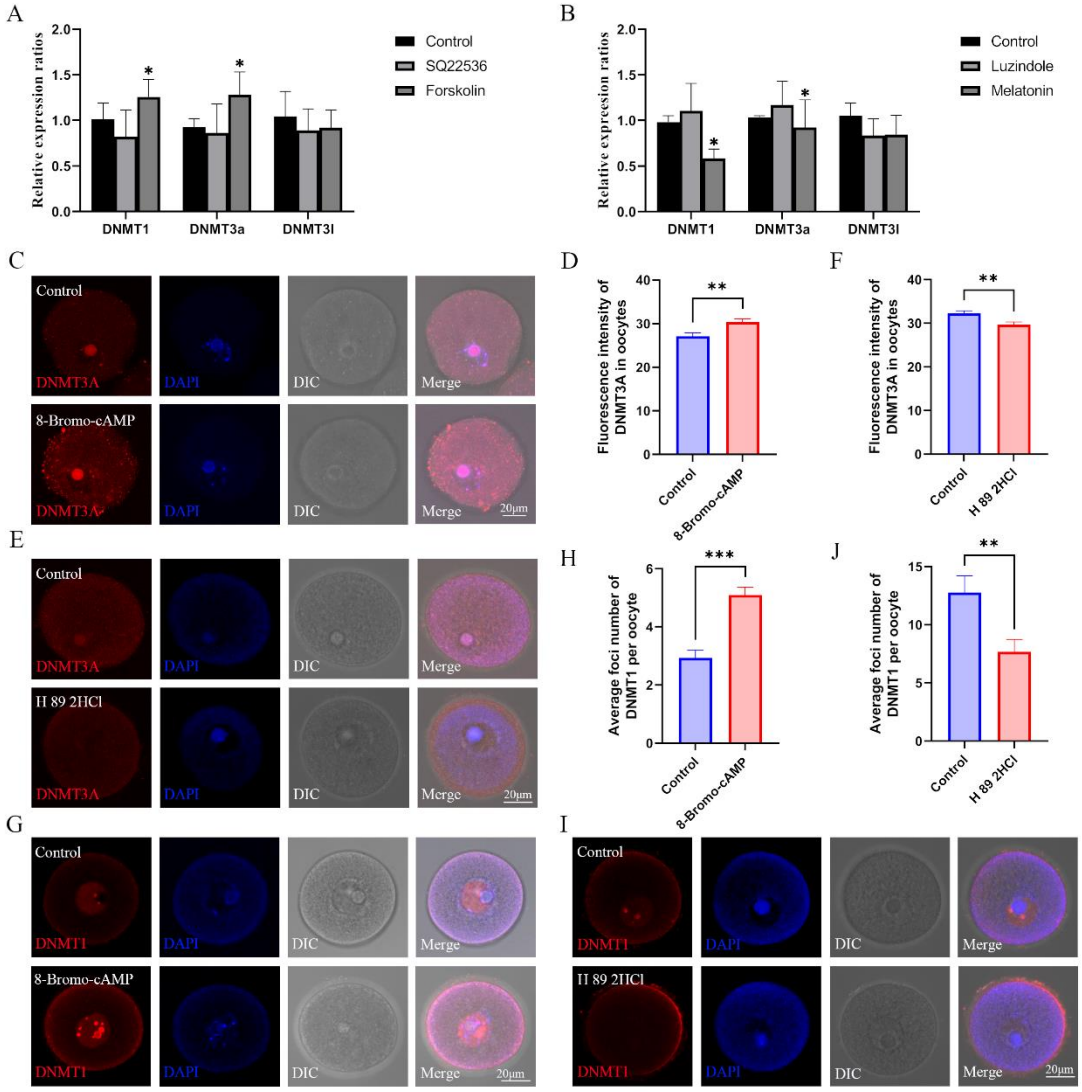

Figure 7 Role of melatonin/cAMP/PKA pathway in the expression of DNMTs.

(A) The expressions of DNMT1, DNMT3a and DNMT3l in oocytes were examined using qPCR after the treatment with SQ22536 and forskolin. *

$p<0.05$.

(B) Relative expressions of DNMT1, DNMT3a and DNMT3l in oocytes were examined using qPCR after the treatment with luzindole and melatonin. * $p<0.05$.

(C) After 8-Bromo-cAMP treatment, the relative expression of DNMT3a in oocytes was examined using immunofluorescence and calculated by Image J (D). ** $p<0.01$.

(E and F) PKA antagonist H 89 2HCL treatment significantly reduced the level of DNMT3a in oocytes examined using immunofluorescence. ** $p<0.01$.

(G and H) DNMT1 localization in oocyte nucleus was examined using immunofluorescence after 8-Bromo-cAMP treatment. *** $p<0.001$.

(I and J) The localization of DNMT1 in oocyte nucleus was reduced by the treatment of PKA antagonist H 89 2HCL. ** $p<0.01$.

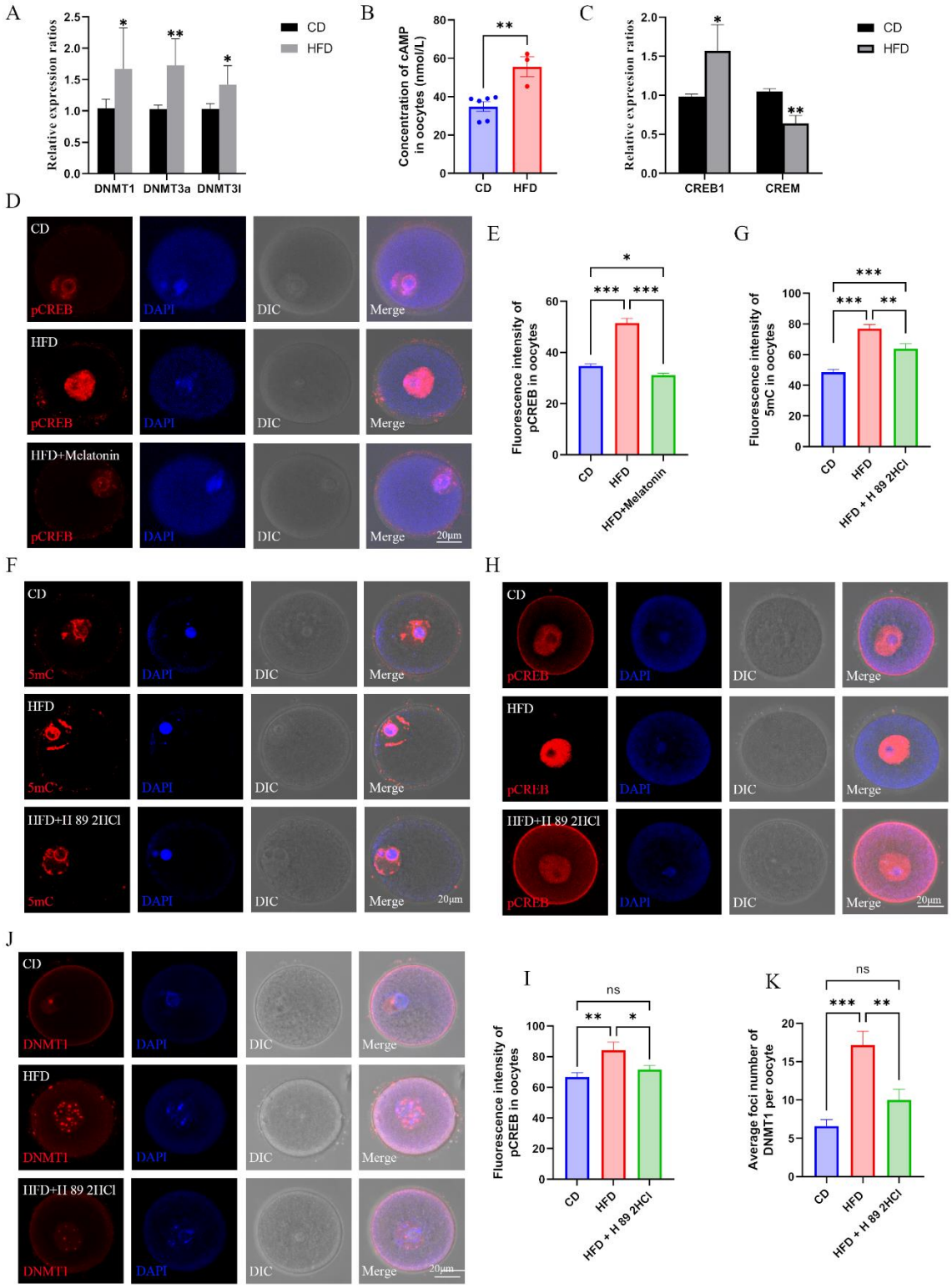

Figure 8 Melatonin regulates DNMTs expression via cAMP/PKA/CREB pathway in HFD oocytes.

(A) Relative expression of DNMT1, DNMT3a, and DNMT3l in HFD

oocytes was examined using qPCR. * $p<0.05$; ** $p<0.01$.

(B) Concentration of cAMP in HFD oocytes was examined using ELISA. ** $p<0.01$.

(C) Relative expressions CREB1 and CREM in HFD oocytes were tested using qPCR. * $p<0.05$; ** $p<0.01$.

(D and E) The level of pCREB1 in oocytes was examined using immunofluorescence, and the relative fluorescence intensity was calculated by Image J (E). HFD, oocytes from obese mice; CD, oocytes from control mice; HFD + melatonin, oocytes from obese mice treated with exogenous melatonin. * $p<0.05$; *** $p<0.001$.

(F and G) PKA antagonist H89 2HCL treatment reduced the methylation level of HFD oocytes. ** $p<0.01$; *** $p<0.001$.

(H and I) The level of pCREB1 in HFD oocytes was also decreased by the treatment of PKA antagonist H89 2HCL. * $p<0.05$; ** $p<0.01$; ns, no statistical significance between groups.

(J and K) PKA antagonist H89 2HCL treatment reduced the localization of DNMT1 in HFD oocytes. ** $p<0.01$; *** $p<0.001$; ns, no statistical significance between groups.